Engineering Structures 302 (2024) 117424

Contents lists available at ScienceDirect

Engineering Structures

journal homepage: www.elsevier.com/locate/engstruct

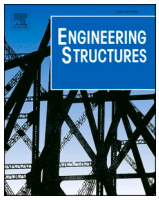

Retrofitting solution for beam-to-column connections of precast reinforced concrete industrial buildings

Hugo Rodrigues [a,*], Nádia Batalha [b], André Furtado [c], António Arêde [b], Romain Sousa [a,d], Humberto Varum [b]

[a] RISCO, University of Aveiro, Portugal
[b] CONSTRUCT, Faculty of Engineering - University of Porto, Portugal
[c] CERIS, Instituto Superior Técnico, Portugal
[d] Vigobloco, AS, Ourém, Portugal

ARTICLE INFO

Keywords:
Retrofit solution
Beam-to-column connections
Cyclic loading
Precast construction
Industrial buildings

ABSTRACT

Precast reinforced concrete building structures are widely used in the Portuguese industrial stock and throughout Europe. Beam-to-column connections are a key component in this type of structure. However, they are also the source of significant damage, as reported in recent earthquakes. Different configurations are common, such as using a dowel, neoprene or just assuming a concrete-to-concrete interface. Both are characterized by a low deformation and strength capacity, presenting a significant vulnerability against seismic actions. Based on this motivation, a novel low-cost and easy-to-apply retrofit connection is herein proposed to reduce this vulnerability. Shear tests were performed to compare the performance of a retrofitted connection with the as-built configuration (i.e. concrete-neoprene interface). The experimental tests showed a good performance of the proposed retrofit solution, emphasizing the importance of this solution in frictional connections to control horizontal displacements. With the use of this solution, it was possible to overcome the resistance obtained in the connections with dowels in the most vulnerable direction, obtaining a 49% increase in the lateral resistance in the most vulnerable direction (loss of support of the beam on the column) concerning that which was verified in the friction-only connection.

1. Introduction

Precast reinforced concrete (PRC) industrial buildings are a common typology in the European industrial park. Recent seismic activity has exposed the vulnerability of these types of structures at both structural and non-structural levels. The damages observed in the beam-to-column connections stand out at a structural level. Connections are usually ensured by friction (i.e. concrete-to-concrete or using neoprene between the concrete interfaces) or by friction combined with a mechanical connector (i.e., dowel). However, the most vulnerable beam-to-column connections are those provided by friction and those with mechanical connectors but designed with low seismic demands in the regions surrounding the dowels [1,2]. Some examples of beam-to-column connection failures are presented in Fig. 1.

Several experimental works emerged to understand this problem [3–8], namely the importance of the diameter and confinement level (spacing of the stirrups) around the dowels, responsible for the development of different types of failures. Psycharis & Mouzakis [3] developed a study focused on the effect of various design parameters on the strength of beam-to-column connections under monotonic and cyclic loading. This work demonstrated the importance of the dowel diameter as the main parameter that influences the connection capacity. In addition, the thickness of the concrete covering the dowels in the direction of loading is pointed out as an important parameter in the connection response. Also, Magliulo *et al.* [2] investigated the shear behaviour of beam-to-column dowel connections. The authors provided a FEM model of the connection validated by experimental tests, and a parametric study was performed varying the dowel diameter and the front and lateral concrete cover. It has been verified that if the lateral and frontal covers are less than 6–7 times the dowel diameter, the failure involves concrete splitting in both cases of force acting against the concrete core and force acting against the concrete cover.

These problems are identified as a result of the lack of knowledge about the seismic response of this type of structures and the design

* Corresponding author.
E-mail address: hrodrigues@ua.pt (H. Rodrigues).

https://doi.org/10.1016/j.engstruct.2023.117424
Received 18 July 2023; Received in revised form 17 October 2023; Accepted 21 December 2023
Available online 28 December 2023

requirements in the prior seismic codes. After performing a literature review and considering the specific properties and characteristics of the industrial building stock [9–15], it was noticed that there was a gap in the study of connections without any mechanical device (dowel), herein called friction connections.

An experimental campaign was then carried out to study, among others, the friction in beam-to-column connections subjected to cyclic pure shear loads [16]. The results found a low strength capacity compared to specimens with dowels (<50%). Based on this poor performance, it was concluded that retrofitting this type of connection is strongly necessary.

Thus, the main goal of this research work is to develop a retrofitting solution for friction connections and perform its experimental validation. Based on the results obtained in the previous experimental investigation [16], it was possible to identify the main limitations of this structural system and define a retrofitting solution that limits the displacements in the direction considered to be the most vulnerable (i.e., scenario where the beam moves away from the column resulting in a decreased contact area between the beam and the column). The retrofit solution was designed based on four main assumptions: *i)* simple detailing leading to a low production cost; *ii)* easy application in the structure to increase scalability in the construction market; *iii)* avoid major interruptions in order not to harm the work activity; and *iv)* introduce a behaviour similar to the connection with the dowels in the pulling direction (see [16]). The proposed retrofit solution will be presented and discussed in this manuscript. Details of the test setup configuration, instrumentation and loading protocol will also be presented. The results will be discussed in terms of force-displacement curves correlated with the damages observed during the tests. Also, the energy dissipation capacity will be discussed. The results of the retrofitted specimens will be compared with the non-retrofitted configuration.

2. Beam-to-column connections retrofitting – an overview

The present section aims to provide an overview of the experimental works developed dealing with the seismic retrofitting of PRC beam-to-column connections, namely on dissipating systems that were investigated in the last years. Belleri *et al.* [17] investigated the use of passive devices on beam-to-column PRC connections to improve seismic performance through energy dissipation during a seismic event. The main goals of the studied devices were to decrease inter-story drift, limit the damages on the base of the columns, and reduce residual drifts. Those devices can be applied at beam-to-column connections of new or existing hinged portal-frame structures. The authors also proposed and implemented a design procedure for these devices in a case study. The assessment of the structure was done using nonlinear analyses. When the devices are included, the results demonstrate a general reduction in the column cross-section dimensions and the quantity of longitudinal rebars.

When compared to traditional RC structures, this type of structure (PRC) has a lower displacement ductility demand, which leads to a design focused on regulating the lateral displacement demand rather than restricting the material strain. [17] The work presented by Belleri *et al.* [17] focuses on reducing seismic lateral displacements and seismic damage in hinged portal-frames by adding beam-to-column connections that can be applied to both new and existing buildings. The beam-to-column devices provide a source of additional damping to the system and a degree of fixity to the beam-to-column joint. The selected devices can be used singly or in combination (acting in parallel), thus allowing the connection to be re-centred after an earthquake.

Moreover, this study also states that the devices in the study are compatible with prestressed elements, which is important in industrial precast buildings, and are activated by additional loads (e.g. seismic loads) giving a restraint at the beam-to-column connection level. The study of the coupled devices demonstrated an increase of the system stiffness, as was expected, due to the transition from a pinned connection to a fixed connection. This retrofitting solution aims to reduce the column damages, the lateral displacement demand and the residual deformations, during a seismic event. The results of the case study show that the use of these devices can lead to a reduction of the column cross-section and the amount of longitudinal reinforcement. Also, it was concluded that the use of both devices leads to a reduction of the column damage, lateral displacement demand and residual deformations.

Morgen & Kurama [18] proposed a friction damper to increase the energy dissipation of unbonded post-tensioned precast concrete building frames in regions with high seismic activity. The application of dampers on precast structures has its primary objective the use of friction as an energy dissipation mechanism to improve the behaviour of the structures to seismic actions. The precast structure already has the benefit of self-centring capability and the ability to perform nonlinear lateral displacements without suffering much structural damage. However, the behaviour of unbonded post-tensioned precast frames on seismic events could result on severe lateral displacements, with the lack of energy dissipation as the source of those large displacements. In this way, the authors describe the passive option of using friction dampers as a solution to improve the seismic behaviour of this type of structures, by increasing energy dissipation. This system uses friction between adjacent metallic surfaces produced by relative beam-to-column interface rotation. To study this system, experimental studies were done through full-scale specimens subject to pseudo-static reversed cyclic loading, varying five different parameters: the beam depth, the initial stress of beam post-tensioning steel, the area of beam post-tensioning steel, the type of friction interface and the damper normal force. The design of the damper pretended not only to ensure the energy dissipation, but also that was an easy device to install and to monitor, and a device that could be installed without disturbing the existing structure and labour activity. As conclusions of the work, the experimental tests demonstrated that

Fig. 1. Examples of beam-to-column connection failures in precast industrial buildings.

dampers improve the moment resistance of the beam, presenting a greater resistance compared with larger beams without dampers. The experimental tests also permitted the comparison between the specimens with and without the friction damper in study, showing the importance of the device: the damper act as the main source of energy dissipation. Also contributes to the shear slip resistance at the beam-to-column interfaces.

Yildirim et al. [19] presented a seismic retrofit of one typical single-story industrial-type PRC building structure in Turkey, using rotational friction dampers. The project consisted of retrofitting twelve PRC buildings. The PRC buildings are widely used in Turkey. That use is related to the low cost, fast assembly and availability of materials in that area. The 1999 Kocaeli and Düzce (Turkey) earthquakes had a great impact on industrial precast structures, leading to a huge economic losses. The Turkey Industrial Park is mainly composed of single-story precast buildings. The retrofit proposal presented by the authors was the first application of energy dissipation devices in Turkey. The retrofit solution applied to the structure, namely on beam-to-column connection, was chosen due to the easy assembly and without closing the building and causing as little disturbance as possible for industrial activities to continue. The expensive cost of the conventional methods of retrofit was the main reason to choose the dampers as the solution to dissipate the energy resulting of the seismic events. Also, additional compression bars between columns were added to guarantee load transferring between frames.

The authors pointed a satisfactory retrofitting using the dampers and the steel members on the precast industrial buildings. Another important point of the retrofitting process is the fact that the process only takes one month to conclude without the need to suspend the labour activities.

Some other devices have been developed and tested to be implemented in the seismic retrofit and upgrading of beam-to-column joints for existing or new structures. Like a self-centring slotted friction device [20], the dissipative devices based on carbon-wrapped steel tubes [21] or the Special Lead Extrusion Damper [22], with the main aim of increasing the energy dissipating potential when compared to the bare cases and reducing the expected damage. Also, different configuration hysteretic devices have been proposed in the literature in recent years [23–25], where the results also demonstrate the efficient behaviour of the proposed solutions, improving the global behaviour of the beam-to-column connection.

From the works previously presented could be concluded that an additional mechanical device is needed at the beam-to-column connections level. These devices will perform better in friction-based beam-to-column connections as a retrofit measure to transferring seismic loads because, in most cases, the friction capacity of this type of connection is not enough if compared to the shear demand at the contact surfaces during a seismic event. If the seismic vertical component is considered, the values of friction are even smaller. In that way, additional components are essential to this connection's typology. The main requirements for the solution selection on the previous works were: *i)* the device dimensions; *ii)* the increase of structural damping without increasing the stiffness; *iii)* a reduced increment in base shear through the building weight; *iv)* an easy assemblage and maintenance; *v)* a structural noninvasive installation; and *vi)* that could be installed without disturbing the labour activity.

3. Testing campaign

3.1. Specimens geometry and reinforcement detailing

The detail of the specimens was established through the work of the typical properties of Portuguese precast industrial buildings presented by Rodrigues et al. [26], namely the column dimensions, corbel length and detail, concrete compressive strength, longitudinal and transverse reinforcement grade, connections dowels, i.e., the number and the diameter, to represent a beam-to-column connection of a typical Portuguese industrial precast building.

The models were constructed at full scale. The column has a rectangular cross-section of $0.50 \times 0.35\ m^2$ with six 16 mm plus four 20 mm diameter bars on the longitudinal reinforcement. On the transversal reinforcement, it was designed 10 mm diameter stirrups spaced at 125 mm. All the specimens have a 25 mm of cover. The columns were cast in a foundation with a rectangular area of $0.80 \times 0.70\ m^2$ and a height of 0.35 m (see Fig. 2). The beam has 1 m of length, with a variable rectangular cross-section of $0.35 \times 0.50\ m^2$ on a 0.60 m of length and on the last 0.40 m has a cross-section of $0.35 \times 0.70\ m^2$ (see Fig. 2), with eight 16 mm plus four 20 mm diameter bars on the longitudinal reinforcement and, on the transversal reinforcement, 10 mm diameter stirrups spaced at 75 mm on the 0.60 m of length being more reinforced in the last 0.40 m.

To replicate a system with a pure shear response, the actuator had to be placed in the exact line of the beam-to-column interface. This required a variable section of the beam which in a real situation does not occur. The measurements of the speciment in study is presente in the Fig. 2c.

Regarding the proposed retrofit solution, it consists on four steel elements of S275 steel joined together: 2 angles of $150\times150\times18\ mm^3$ (one placed above that connects to the beam – 'A′ part – and another placed below that connects to the corbel of the column – 'C′ part), two threaded rods of 310 mm in length with 16 mm of diameter and a plate welded to the bars that makes the connection to the upper part – 'B′ part. In Fig. 3 are presented the detailed drawings of each part with the respective measurements. Fig. 2c) is complementary.

The measurements were established based on the design done so that the steel angle placed on the column's corbel ('C' part) or the threaded rods reached the yield strength for a force similar to the one obtained for the specimen with centered dowels (SPC_c1_150 kN).

Table 1 summarizes the properties specimens in study, specifically the specimens name, the neoprene pads, the axial load applied, the dowels (number, diameter and location) and retrofit, if present. The 'c′ refers to the longitudinal distance from the internal face of the column to the center of the dowel. The option for two neoprene pads intended to mimic a solution commonly employed in current. Regarding the nomenclature the name adopted to each specimen was the original one ("SPC_xx_yy"), already described in [16], plus a "_R" in the end.

3.2. Testing setup and load protocol

The test setup used in this testing campaign was the one previously presented in [16] with the original specimens with a small adjustment.

Initially, was considered the same setup used in the first part of the experimental campaign, but after the first test it was concluded that it would not work in the same way. From Fig. 4a), it can be observed that during the test, the beam excessive rotation was evident due to the retrofit solution that introduced a force that ended up pulling the beam towards itself, ending up rotating around the axis perpendicular to the plane that was see in the figure. This rotation created an increase in tensions on the edge of the corbel, causing fragility and ending up with cracks in that same area (Fig. 4b). The retrofit turned out not to be effective in this situation because the test ended prematurely as the damage appeared precisely in that area of the corbel and the corbel ended up collapsing through the detachment of the concrete (Fig. 4b).

In this sense, it was considered to support the beam so that when the actuator is pulling the beam it does not rotate, which is an approximation to the real situation. The setup was developed to prevent the rotation at the joint and the tests were performed for pure shear behavior of the connection. In this way, the phenomena associated with the shear deformation alone could be studied. It should be noted, however, that in real structures there might be rotation at the joints, caused mainly by the deflection of the columns. Large joint rotations may reduce the overall shear resistance of the connections, as observed in other experimental tests [27,28]. Fig. 5a) shows the modified scheme, adding the modified

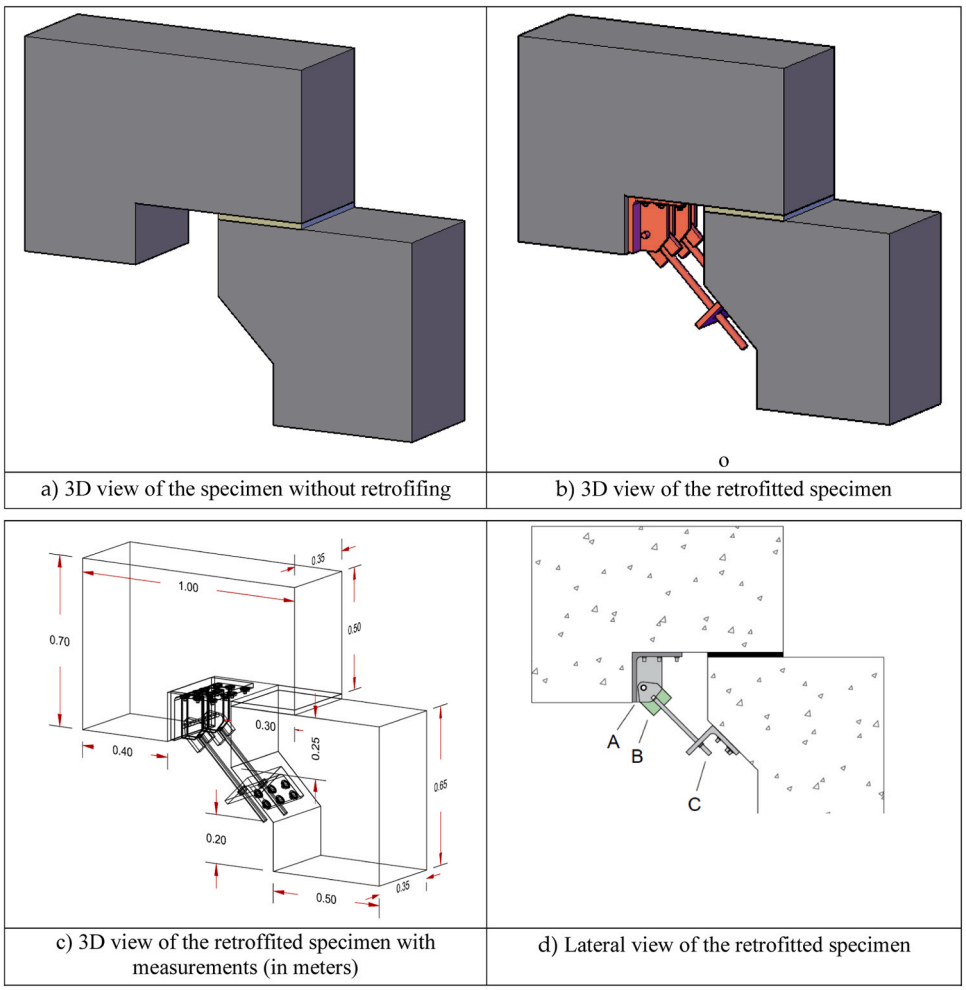

Fig. 2. Retrofitted specimen in study.

part in red. In addition to this particularity, all the rest of the setup was maintained. Fig. 5b) shows the modified setup.

The horizontal actuator applied displacement-controlled lateral cyclic loading according to the displacement history shown in Fig. 6, at a constant velocity of 0.2 mm/s.

The instrumentation schematic layout adopted is presented in Fig. 7. Twelve transducers were used: nine placed at the top and bottom of the beam's front and two others in the top and bottom of the column. An additional transducer was placed at the foundation level to control the lift/rotation of the foundation. Also an inclinometer was placed on the top beam to control a possible beam rotation.

4. Experimental results

The main experimental results obtained in this experimental campaign are herein presented in this section, starting with the discussion of the force-displacement hysteretic curves of the specimens SPC_i2_150 kN with the retrofit solution applied SPC_i2_150kN_R1 and SPC_i2_150kN_R2. Afterwards the results will be discussed in terms of relative stiffness, maximum strength and corresponding displacement, dissipated energy per cycle and cumulative energy dissipation. This comparison is important to better characterize the effect of the retrofit solution. Also, the damages observed during the experimental test will be presented and discussed, and once again compared with the reference specimen (already presented in [16]) SPC_i2_150 kN.

4.1. Damage observation

The behaviour of the retrofitted specimen was consistent throughout the experimental tests and can be characterized by two main features. First, there were no observed damages in the beam and column, indicating a lack of concrete cracking or spalling. Second, as the pull displacements increased, there was a progressive increase in the deformation of the bars until they eventually failed. The main damages of the retrofitted specimen are presented in Fig. 8. It was observed that after the failure of one of the bars, the other one immediately reached the rupture due to the stress concentrations caused by the quick increment due to the stress redistribution. The position of the failure varied in both bars, being one of the ruptures located near the beam L-shape steel profile and the other one near to the column L-shape steel profile. From the perspective of the retrofitting design concept, this behavior aligns with expectations. The retrofitting effectively prevented damage in the reinforced concrete (RC) elements, and instead, the damage was concentrated solely on the steel bars that connect the L-shaped steel profiles, serving as energy dissipators. In summary, the retrofitting technique successfully protected the RC elements, while allowing the steel bars to absorb and dissipate energy, thus demonstrating the desired behavior as intended by the retrofitting design concept presented bellow.

The damage observed in the reference specimen (i.e., specimen only with neoprene placed between the concrete interfaces) is depicted in Fig. 9. During the test, minor damage was detected at the column level, while no visible damage was observed in the beams. Neoprene is an

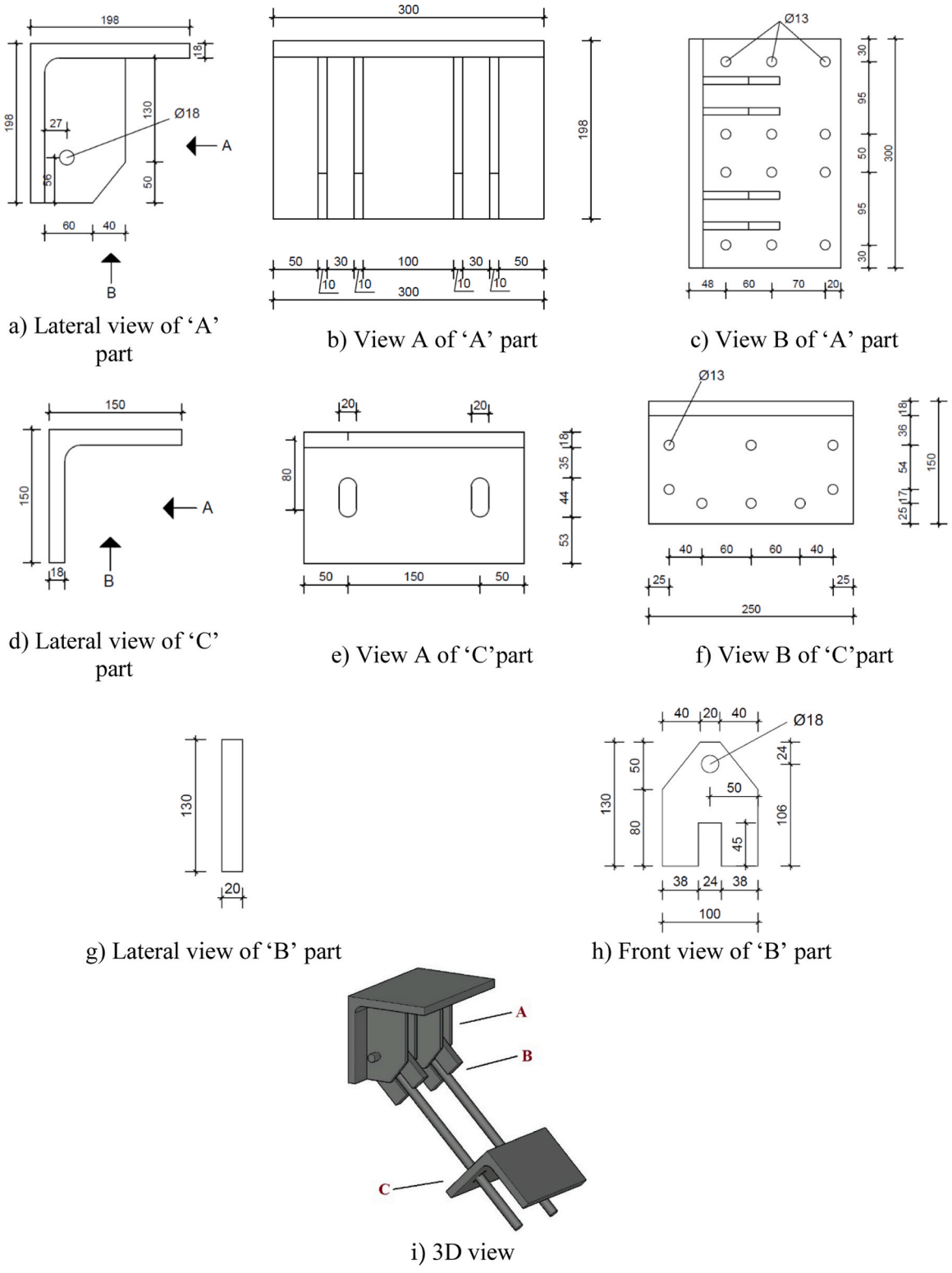

Fig. 3. Parts that constitute the retrofit solution a), b) and c) Part 'A'; d) e) and f) Part 'C'; g) and h) Part 'B' (measurements in mm); i) 3D view.

elastic material capable of undergoing significant elastic deformation under substantial loading. As the shear displacement at the interface increases, the adhesion stress can approach its limit, leading to rupture or sliding phenomena between the concrete surface and the neoprene pad. Furthermore, deterioration of the neoprene placed between the concrete interfaces was observed, along with slight concrete detachment in the upper zone of the column's corbel.

4.2. Force-displacement response

The hysteresis curves from the conducted tests are illustrated in Fig. 10. The results of the reference specimen SPC_i2_150 kN are presented first in Fig. 10a) to provide the reader with an understanding of the as-built behavior response, specifically regarding important parameters such as initial stiffness, maximum strength, yielding plateau,

Table 1
Characteristics of the specimens under analysis.

ID	Dowel [mm]	Neoprene pads thickness [mm]	Axial Load [kN]	c [mm]	Retrofit
SPC_i2_150kN	-	2 × 10 mm pad	150	-	-
SPC_i2_150kN_R1	-	2 × 10 mm pad	150	-	Yes
SPC_i2_150kN_R2	-	2 × 10 mm pad	150	-	Yes

and stiffness degradation. From its analysis, it is evident that the shape of the hysteresis curve remains relatively constant throughout the test. It begins with an initial stiffness of 11.52 kN/mm and gradually reaches the maximum shear strength of 86.27 kN at a displacement of 10.74 mm in the pull direction, and 79.43 kN at a displacement of 13.03 mm in the push direction. The peak load in the pull direction was approximately 9% higher than in the push direction, while the peak load displacements were similar in both directions.

After reaching the peak load, the shear load experiences a slight decrease before stabilizing at around 60–65 kN until the end of the test. This behavior can be attributed to the friction between the neoprene and the concrete interfaces, which has been extensively discussed in previous works by other researchers. Additionally, the hysteresis plot indicates an approximate symmetry in the response, with similar force values observed in both the push and pull directions.

It is worth noting that the unloading stiffness for displacements exceeding 15 mm is approximately 25% lower than the values observed for displacements below 15 mm. This discrepancy can once again be attributed to the frictional forces. Unfortunately, the test was terminated for a displacement around 45 mm due to the limitation of the hydraulic atuator, and further information beyond this point is unavailable.

The force-displacement curve for specimen SPC_i2_150kN_R1 is presented in Fig. 10b). Before delving into the discussion of the results, it is important to provide context regarding what transpired during this test. Initially, the test exhibited regular behaviour. However, for displacements exceeding 10 mm in the pull direction, it was observed that the bars were not securely fixed to the L-shaped steel profiles. Consequently, a decision was made to halt the test at a displacement of 15 mm to rectify the connection. Following this intervention, the test was resumed until failure of the reinforcing bars occurred.

This development clearly explains the peculiar shape of the curve observed in the pull direction, where a decrease in shear strength between 10 mm and 20 mm is noticeable. However, it should be emphasized that since the objective of this test was to evaluate the effectiveness of the proposed retrofitting solution in enhancing strength and energy dissipation capacity, it can be concluded that this case did not compromise the overall objective. Analyzing the hysteresis curve, it becomes apparent that the shape is asymmetric instead of what was observed in the reference specimen SPC_i2_150kN. This discrepancy in behaviour can be attributed to the active role of the retrofitting system solely in the pull direction. In other words, the strength significantly increases only when displacements are negative, leading to bar failure. Conversely, in the push direction, the load remains relatively constant at approximately 65 kN. It is also noteworthy that for low displacement demands in the push direction, the shear force level matches that observed for larger displacements. This behaviour was not observed in the reference specimen.

a) Beam rotation b) Corbel damages

Fig. 4. Damage to specimens with initial setup (before adjustments).

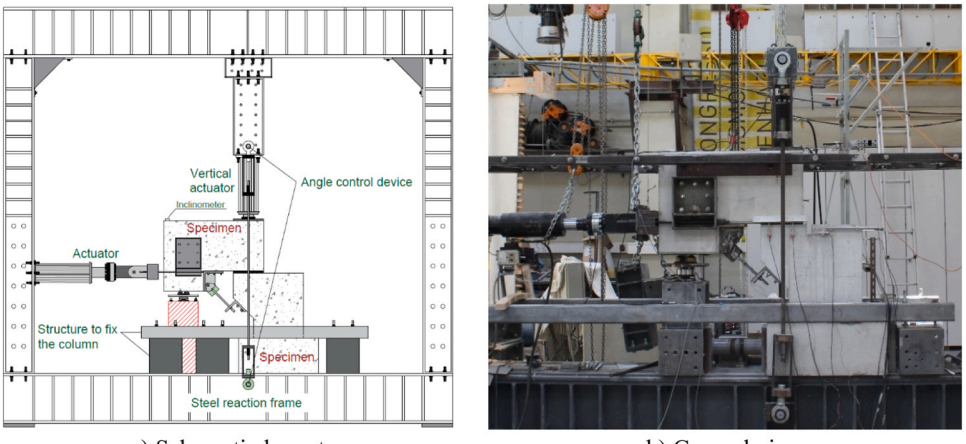

a) Schematic layout b) General view

Fig. 5. Testing setup for retrofitted specimens at LESE laboratory.

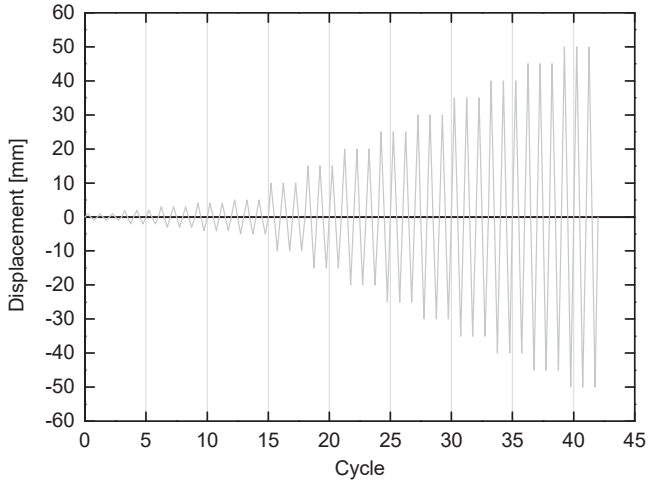

Fig. 6.. Displacement history applied on the cyclic tests.

Regarding the key response parameters, the initial stiffness in the push direction was measured at 8.80 kN/mm, while the peak strength reached 66.80 kN at a displacement of 24.53 mm. In the pull direction, the peak load registered − 175.39 kN at a corresponding displacement of 30.93 mm, which coincided with the occurrence of bar rupture.

The force-displacement curve for specimen SPC_i2_150kN_R2 is presented in Fig. 10c). Before this test, special attention was given to ensure proper fixation of the retrofitting bars, aiming to prevent the recurrence of the previous specimen. Once again, asymmetry is observed in both the push and pull directions. In the push direction, similar to what was observed in specimen SPC_i2_150kN_R1, the shear strength remains constant at around 70.6 kN. On the other hand, in the pull direction, a linear elastic behaviour can be observed up to a displacement of 13 mm, followed by the yielding of the bars and eventually their rupture. The initial stiffness of the specimen was approximately 29.82 kN/mm. The maximum strength reached 78.81 kN at a displacement of 6.52 mm (push direction) and − 177.08 kN at a displacement of − 20.43 mm (pull direction).

The envelopes of the force-displacement curves are presented in Fig. 10d), where it is possible that the initial stiffness of the specimens SPC_i2_150kN_R2 and SPC_i2_150kN was 50% and 65% higher than SPC_i2_150kN_R1. The peak load in the push direction occurred around the same displacements in the case of the specimens SPC_i2_150kN_R2 and SPC_i2_150kN (around 6 mm), instead of what was observed in the SPC_i2_150kN_R1 (25 mm). Concerning the pull direction, the retrofitting was very efficient since it improved significantly the strength capacity of the beam-to-column connection.

The overlapping force-displacement curves are illustrated in Fig. 11, providing insights into the effectiveness of the retrofitting solution. By comparing the responses of the reference specimen SPC_i2_150kN with the retrofitted specimens SPC_i2_150kN_R1 and SPC_i2_150kN_R2, as shown in Fig. 11a) and Fig. 11b), the following observations can be made: i) In the push direction, the behavior remains similar across all specimens; ii) The retrofitting solution significantly enhances the stiffness and strength in the pull direction. This is evident from the curves of SPC_i2_150kN_R1 and SPC_i2_150kN_R2, which exhibit higher values compared to the reference specimen SPC_i2_150kN; iii) The unloading stiffness is higher in the pull direction, primarily due to the retrofitting. This can be observed by comparing the descending portions of the curves, indicating a greater resistance to deformation during unloading. By analyzing the overlapping curves in Fig. 11, the positive impact of the retrofitting solution becomes evident, particularly in terms of increased stiffness, strength, and improved unloading behavior in the pull direction.

When comparing the retrofitted specimens depicted in Fig. 11c), it is evident that their behavior in the push direction is quite similar. However, notable differences arise in the pull direction. The key distinction is that specimen SPC_i2_150kN_R2 achieves higher shear loads for lower displacement demands compared to specimen SPC_i2_150kN_R1. It appears as if the curve of SPC_i2_150kN_R1 is a shifted version of the curve observed in specimen SPC_i2_150kN_R2 for larger displacements. This discrepancy can be attributed to the interruption of the test for specimen SPC_i2_150kN_R1 due to the inadequate fixation of the reinforcing bars. Consequently, the behaviour and response of SPC_i2_150kN_R1 may have been affected, resulting in a lower initial stiffness value compared to the other specimens. The interruption of the test and subsequent corrective measures may have influenced the overall performance and shape of the curve in SPC_i2_150kN_R1.

The evolution of stiffness degradation (Fig. 12a)) was assessed by comparing the peak-to-peak secant stiffness of the first cycle for each imposed peak displacement in the positive and negative directions, aiming to understand the impact of the retrofitting.

Upon analyzing the relative stiffness in the push (positive) direction, it is evident that the curves exhibit a high degree of similarity. This can

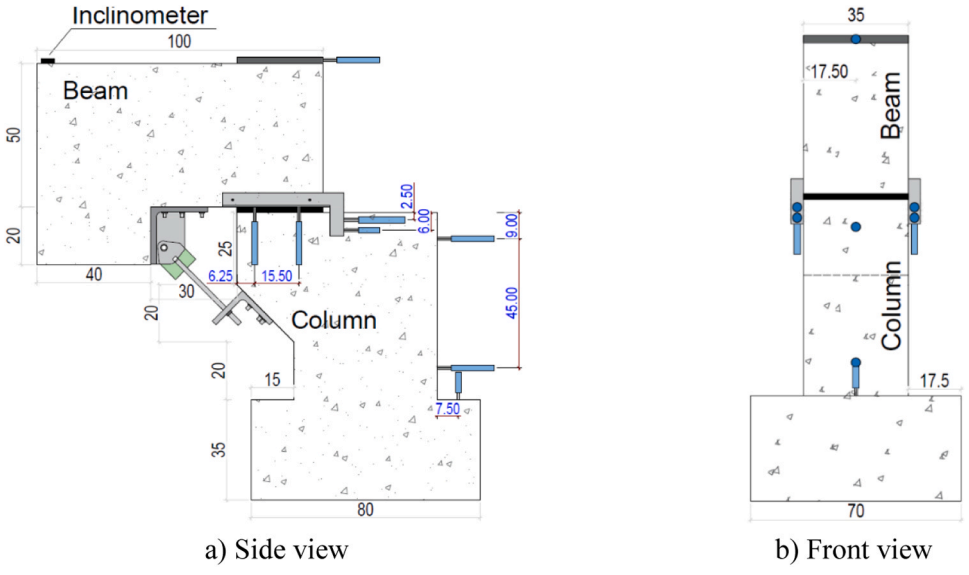

Fig. 7. Displacement instrumentation scheme adopted in the retrofitted specimens along with the general measures of the specimens (units in cm).

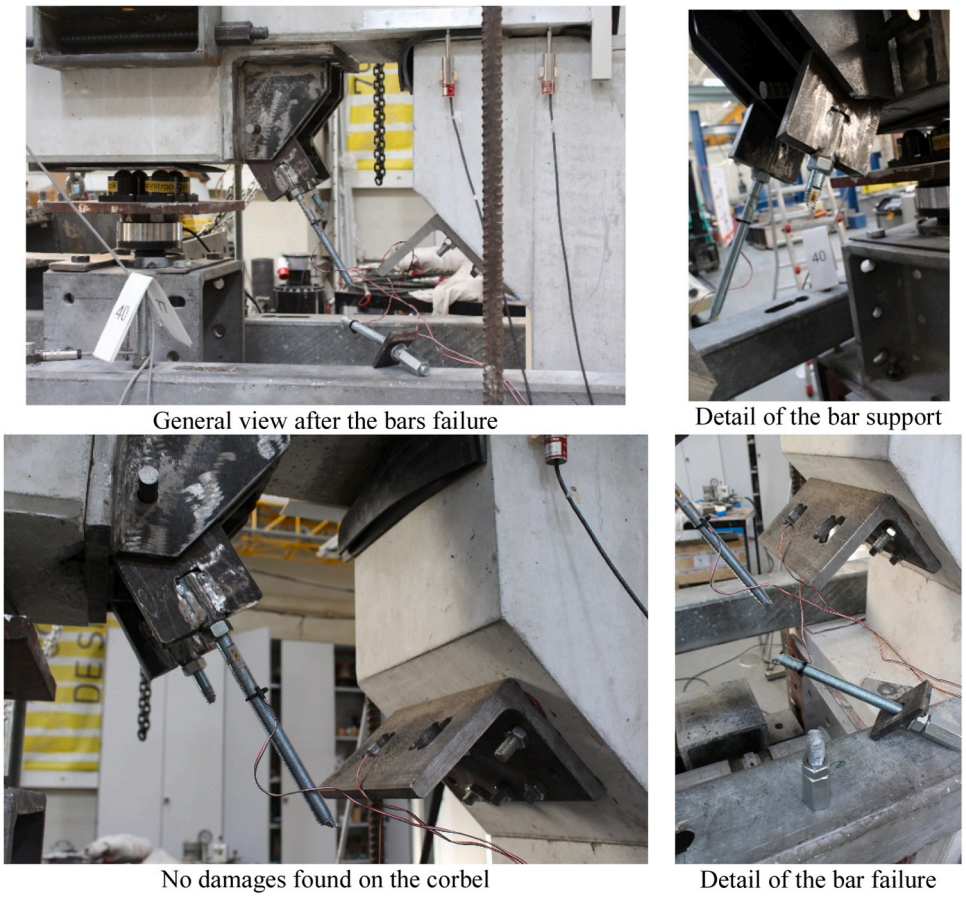

Fig. 8. Damages observed in the retrofitted specimens SPC_i2_150kN_R1 and SPC_i2_150kN_R2.

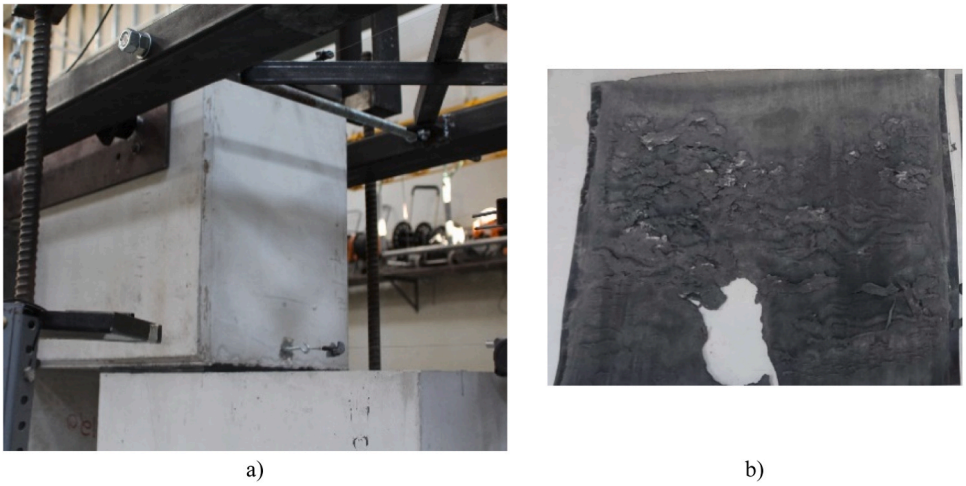

Fig. 9. Damages observed in the nonretrofitted specimens SPC_i2_150kN.

be attributed to the fact that the retrofitting system remains inactive when the specimen undergoes positive displacements. Minor differences ranging from 5% to 15% can be observed among the curves. Overall, in the push direction, it can be concluded that for low displacement demands (up to 20 mm), the specimen SPC_i2_150kN_R1 experience a higher stiffness degradation, followed by SPC_i2_150kN_R2 and SPC_i2_150kN. However, for displacements exceeding 20 mm, there is a reversal in positions, with SPC_i2_150kN_R2 exhibiting the highest stiffness degradation, followed by SPC_i2_150kN and SPC_i2_150kN_R1.

Regarding the pull (negative) direction, the retrofitting system effectively prevents stiffness degradation when compared to the reference specimen. For instance, SPC_i2_150kN experiences an 80% stiffness degradation up to − 5 mm. In contrast, SPC_i2_150kN_R1 only demonstrates a reduction of 70% for displacements larger than − 30 mm, and SPC_i2_150kN_R2 reaches an 80% reduction for the maximum displacement of − 20 mm.

In Fig. 12b) it is presented a comparison between the maximum strength reached by the three specimens in both push and pull directions. Concerning the push directions, the results are very similar being the higher shear strength reached by SPC_i2_150kN with

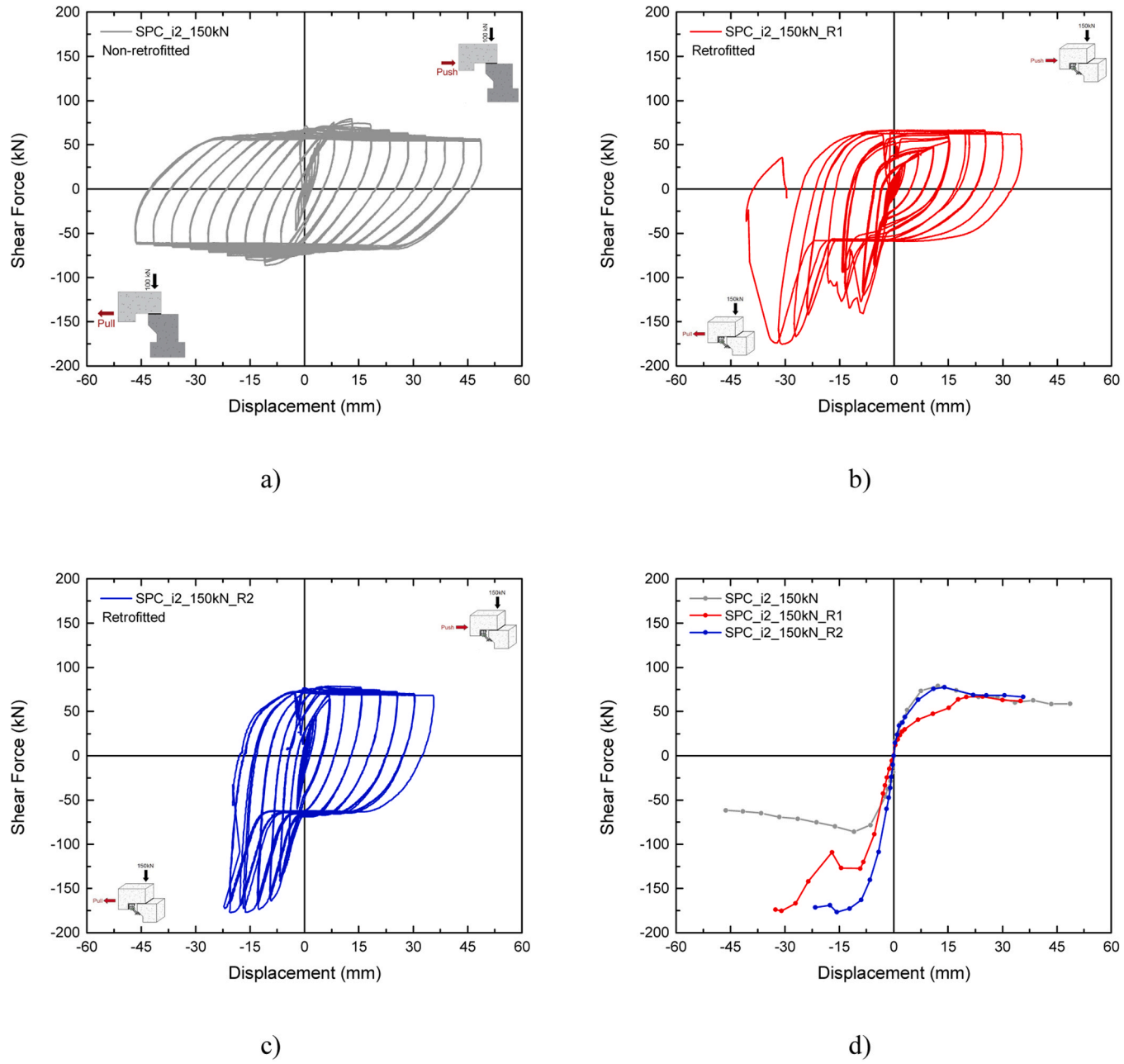

Fig. 10. Force-displacement curves: a) SPC_i2_150kN b) SPC_i2_150kN_R1; c) SPC_i2_150kN_R2 and d) envelope curves comparison.

79.43 mm, about 16% higher than SPC_i2_150kN_R1 and 1% higher than SPC_i2_150kN_R2.

4.3. Cumulative energy dissipation

In the design process of repair and retrofit, one of the primary objectives is to enhance the capacity of structures and increase their energy dissipation capacity when subjected to earthquakes, without significant strength reduction. The dissipated energy can be quantified by summing the energy dissipated in both the push and pull directions. The evolution of cumulative energy dissipation for each specimen, as the displacement demand increases, is illustrated in Fig. 13. The plotted values represent the accumulated dissipated energy at the conclusion of the third cycle of repetition for each imposed displacement peak, as per the defined loading conditions outlined in sub-section 3.2.

From the analysis of the energy dissipated for each cycle, it can be concluded that the retrofitting contributes to a consistent increase of the energy dissipation, which is basically due to the area of the half-cycle along the pull direction. A similar shape can be noticed in the plots of the specimens SPC_i2_150kN_R1 and R2, shown in Fig. 13b) and Fig. 13c), respectively. The main difference compared to the reference specimen is that for large displacement demands, the energy dissipation per cycle is constant.

In Fig. 14a) presents the cumulative energy dissipation of the three specimens. Three specific stages were defined for discussion: i) stage 1 corresponding to the end of the linear elastic branch (~15 mm); ii) stage 2 corresponding to the end of the test of the specimen SPC_i2_150kN_R1; and iii) stage 3 corresponding to the end of the test of the specimen SPC_i2_150kN_R2. For a better understanding of the retrofitting effect, it is plotted in Fig. 14b) the ratio between the cumulative energy dissipation of the retrofitted specimen and the reference one for each stage. Also, this plot allows to compare the cumulative energy dissipation for the same displacement demands.

For lower displacement demands (lower than 15 mm) the behaviour

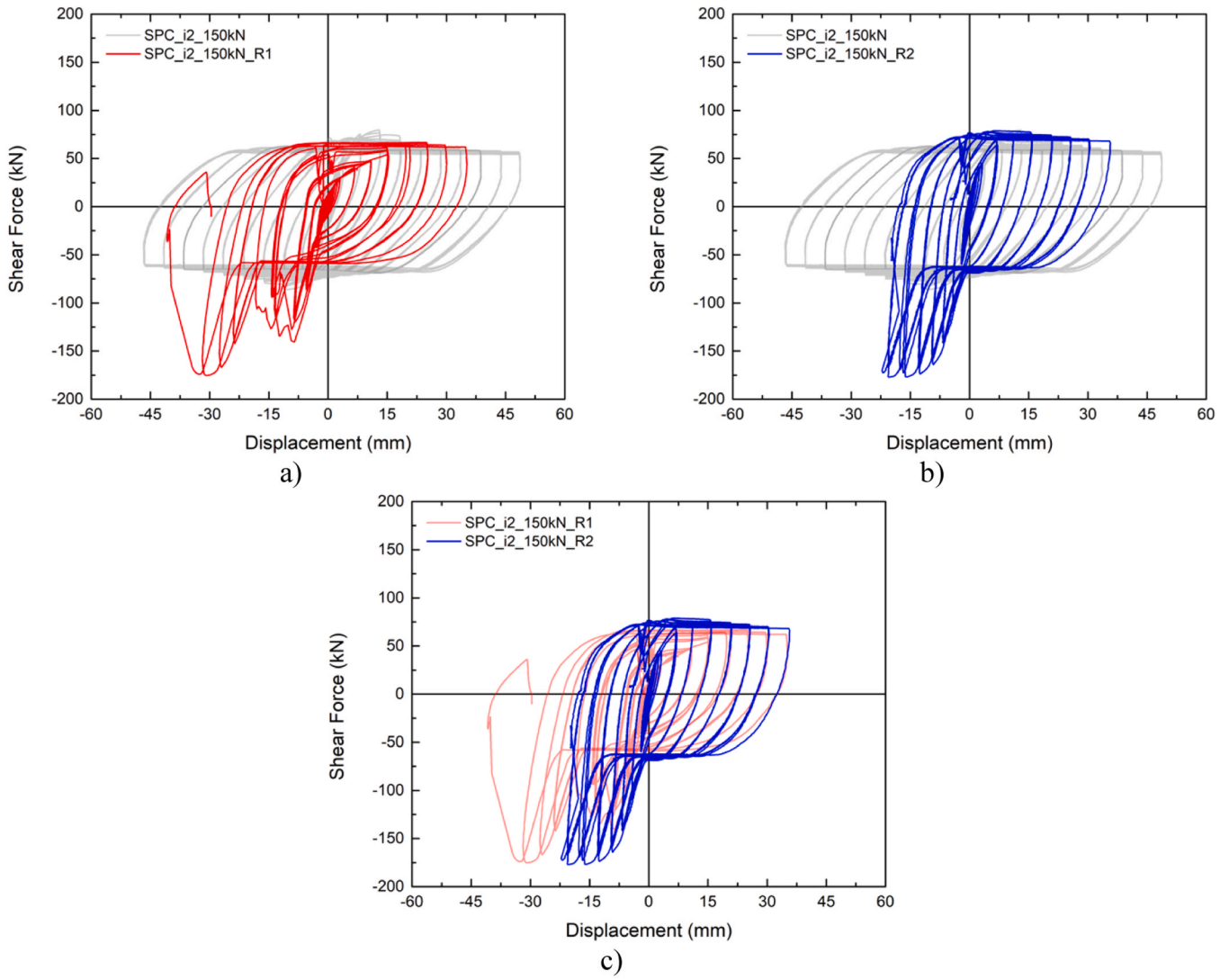

Fig. 11. Comparison between force-displacement curves: a) SPC_i2_150kN vs SPC_i2_150kN_R1 b) SPC_i2_150kN vs SPC_i2_150kN_R2; and c) SPC_i2_150kN_R1 vs SPC_i2_150kN_R2.

of the retrofitted specimens was very similar dissipating 200% higher energy than the reference one. Then, until reach the stage 2 there is a reduction of the energy dissipation of the specimen SPC_i2_150kN_R1 until captures the evolution of the reference specimen. On the opposite, the specimen SPC_i2_150kN_R2 dissipated 50% higher energy than the reference specimen. Then, the trend kept constant, and stage three was reached with the retrofitted specimen SPC_i2_150kN_R2 dissipating about 20% higher energy than the reference specimen.

5. Conclusions

The main purpose of this research work was to study retrofitting connection solution for PRC beam-to-column connections commonly used in Portuguese industrial stock and throughout Europe. These connections have shown vulnerability to seismic actions, leading to significant damage in recent earthquakes. The proposed retrofit solution aims to address this vulnerability by providing a low-cost and easy-to-apply connection that enhances the deformation and strength capacity.

Cyclic tests were conducted to compare the performance of the retrofitted connection with the as-built configuration, which involved a concrete-neoprene interface. The experimental results revealed several key findings. Firstly, the retrofitted specimens exhibited no damage in the beam and column, indicating the successful protection of the reinforced concrete elements. Instead, the damage concentrated solely on the steel bars connecting the L-shaped steel profiles, serving as energy dissipators as intended by the retrofitting design concept.

Comparing the retrofitted specimens with the reference one, it was observed that the retrofitting solution significantly increased the stiffness and strength in the pull direction. The hysteresis curves exhibited asymmetry due to the active role of the retrofitting system in the pull direction, resulting in higher shear loads and improved unloading behaviour. In terms of stiffness degradation, the retrofitted specimens showed superior performance in preventing degradation compared to the reference specimen, particularly in the pull direction.

The cumulative energy dissipation analysis demonstrated the effectiveness of the retrofitting solution. The retrofitted specimens consistently exhibited higher energy dissipation, primarily due to the increased area of the half-cycle along the pull direction. The retrofitted specimen SPC_i2_150kN_R2 demonstrated the highest energy dissipation among the retrofitted specimens, surpassing the reference specimen by approximately 20% at the end of the test.

Overall, the experimental results validate the effectiveness of the proposed retrofit connection in enhancing the deformation and strength capacity of PRC beam-to-column connections. The retrofitting solution successfully protected the reinforced concrete elements while allowing the steel bars to absorb and dissipate energy. This research contributes

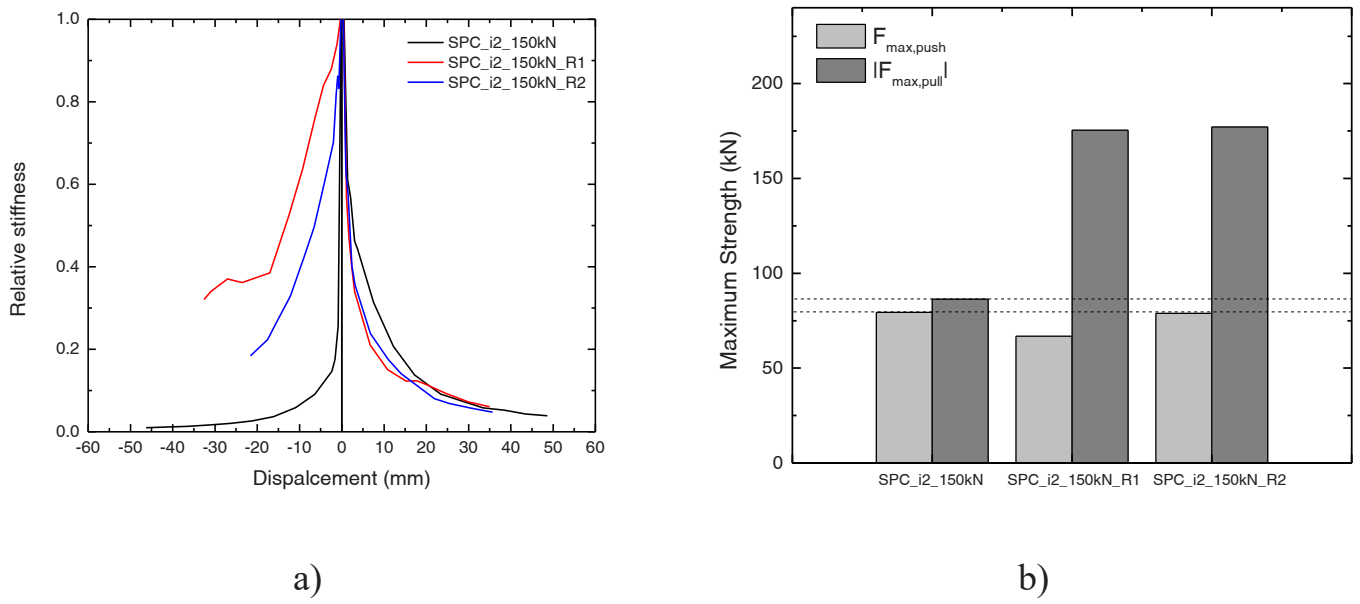

Fig. 12. Comparison between: a) relative stiffness and b) maximum strength.

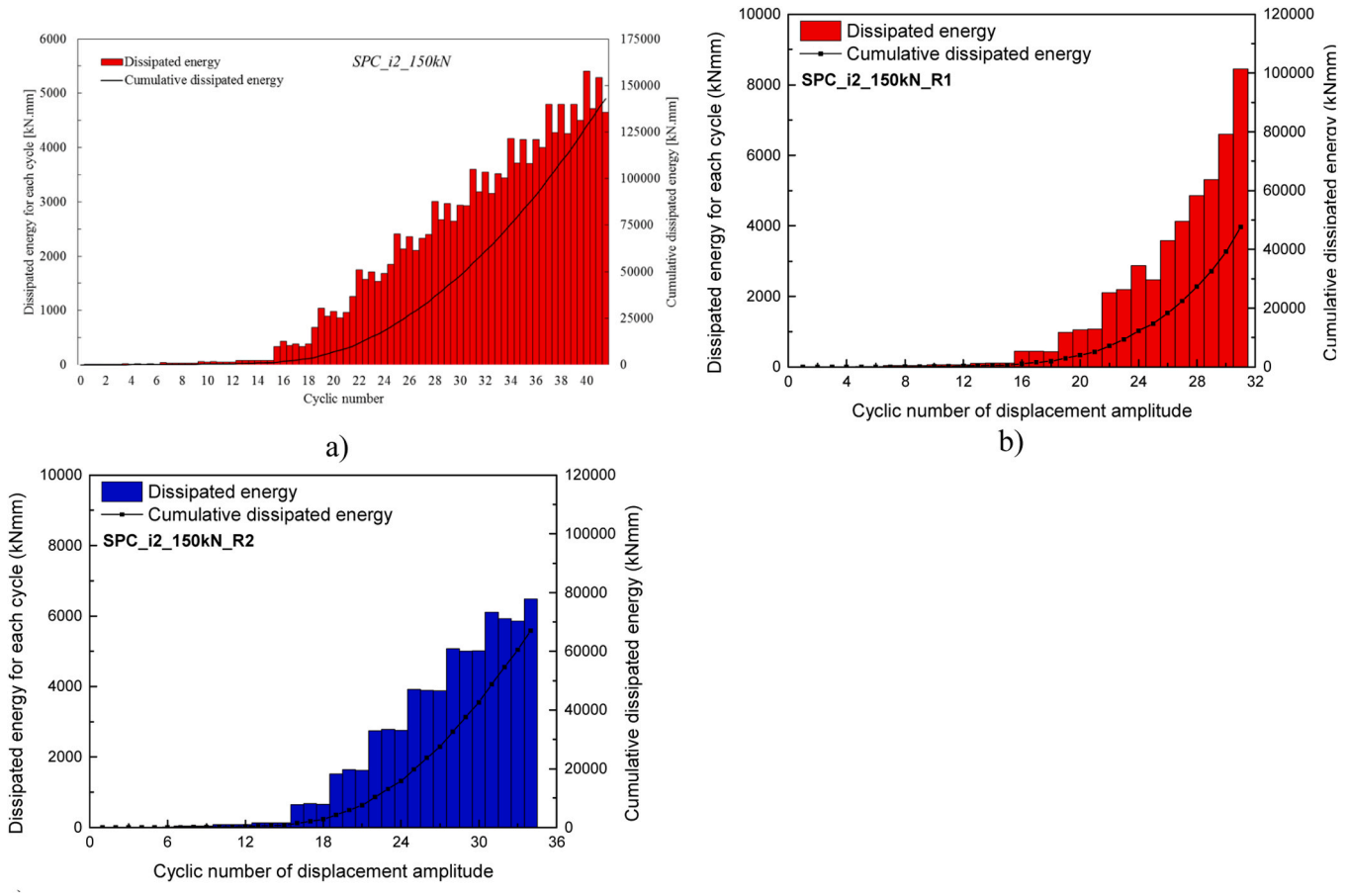

Fig. 13. Dissipated energy per each cycle: a) SPC_i2_150kN b) SPC_i2_150kN_R1; and c) SPC_i2_150kN_R2.

to the development of cost-effective and efficient retrofit techniques for improving the seismic performance of PRC building structures, ultimately enhancing their resilience and safety in seismic events.

The study also revealed limitations and areas for future work. During one of the tests, the bars were not securely fixed to the L-shaped steel profiles, leading to a decrease in shear strength in the pull direction. Although this situation did not compromise the overall objective of evaluating the retrofitting solution's effectiveness, it highlighted the importance of proper connection fixation. Future work should focus on improving the connection design and implementation to ensure reliable

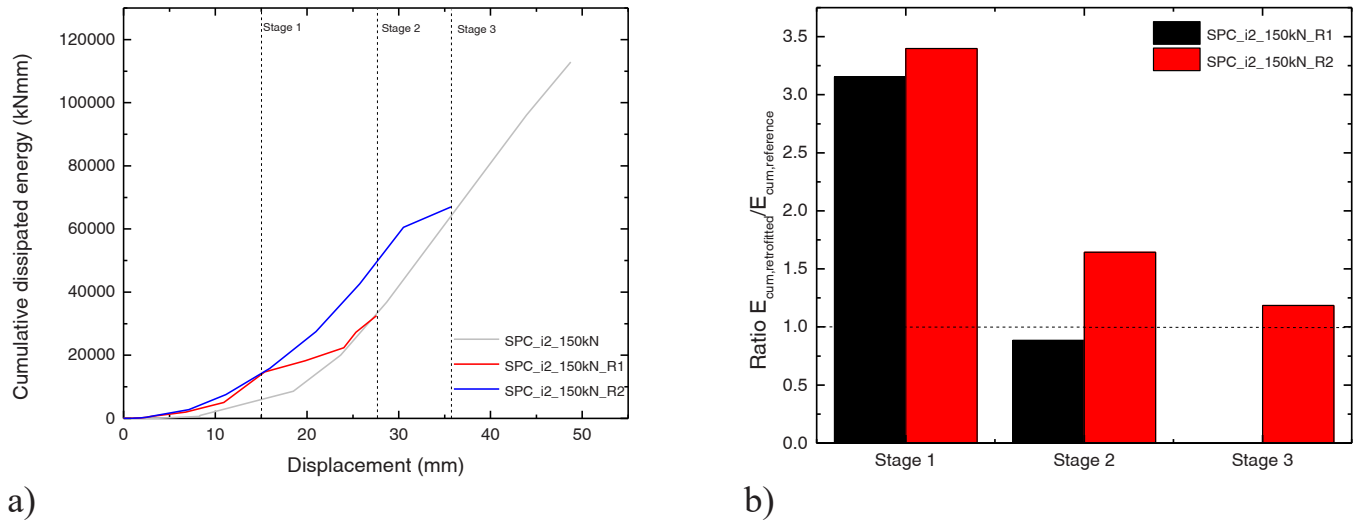

Fig. 14. Comparison between a) cumulative dissipated energy and b) ratio between cumulative energy dissipation of retrofitted specimens and reference specimens per stage.

and consistent performance.

Overall, the proposed retrofitting technique demonstrated promising results in protecting the RC elements and enhancing the energy dissipation capacity of PRC beam-to-column connections. With further refinement and evaluation, this low-cost and easy-to-apply solution has the potential to contribute to the seismic resilience of PRC structures. Future research efforts should aim to optimize the connection design, address the fixation challenges, and conduct tests with larger displacement demands to assess the retrofitting solution's performance under more severe seismic actions.

CRediT authorship contribution statement

Sousa Romain: Conceptualization, Investigation, Methodology. **Arêde António:** Conceptualization, Investigation, Methodology, Resources. **Varum Humberto:** Conceptualization, Investigation, Supervision. **Rodrigues Hugo:** Conceptualization, Formal analysis, Funding acquisition, Investigation, Supervision, Writing – review & editing. **Furtado André :** Formal analysis, Investigation, Methodology, Writing – original draft. **Batalha Nádia:** Formal analysis, Investigation, Writing – original draft.

Declaration of Competing Interest

None.

Data availability

Data will be made available on request.

Acknowledgements

This work was supported by the Foundation for Science and Technology (FCT) – Aveiro Research Centre for Risks and Sustainability in Construction (RISCO), Universidade de Aveiro, Portugal [FCT/UIDB/ECI/04450/2020]. This work was also financially supported by: Project POCI-01-0145-FEDER-007457 – CONSTRUCT – Institute of R&D In Structures and Construction funded by FEDER funds through COMPETE2020 – Programa Operacional Competitividade e Internacionalização and by national funds through FCT – Fundação para a Ciência e a Tecnologia. The authors are also grateful for the Foundation for Science and Technology's support through funding UIDB/04625/2020 from the research unit CERIS. The second author acknowledged to FCT – Fundação para a Ciência e a Tecnologia namely through the PhD grant with reference SFRH/BD/139723/2018.

References

[1] Belleri A, Brunesi E, Nascimbene R, Pagani M, Riva P. Seismic performance of precast industrial facilities following major earthquakes in the Italian territory. J Perform Constr Facil 2015:1–31.
[2] Magliulo G, Ercolino M, Cimmino M, Capozzi V, Manfredi G. FEM analysis of the strength of RC beam-to-column dowel connections under monotonic actions. Constr Build Mater 2014;69:271–84. https://doi.org/10.1016/j.conbuildmat.2014.07.036.
[3] Psycharis IN, Mouzakis HP. Shear resistance of pinned connections of precast members to monotonic and cyclic loading. Eng Struct 2012;41:413–27. https://doi.org/10.1016/j.engstruct.2012.03.051.
[4] Psycharis I.N., Mouzakis H.P., Carydis P.G. Experimental Investigation of the Seismic Behaviour of Precast Structures with Pinned Beam-to-Column Connections in Role of Seismic Testing Facilities in Performance-Based Earthquake Engineering. 2012. https://doi.org/10.1007/978–94-007–1977-4.
[5] Fischinger M., Zoubek B., Kramar M., Isaković T. Cyclic response of dowel connections in precast structures. 15th World Conference on Earthquake Engineering 2012.
[6] Zoubek B, Isakovic T, Fahjan Y, Fischinger M. Cyclic failure analysis of the beam-to-column dowel connections in precast industrial buildings. Eng Struct 2013;52:179–91. https://doi.org/10.1016/j.engstruct.2013.02.028.
[7] Zoubek B, Fischinger M, Isakovic T. Estimation of the cyclic capacity of beam-to-column dowel connections in precast industrial buildings. Bull Earthq Eng 2015. https://doi.org/10.1007/s10518-014-9711-0.
[8] Capozzi V., Magliulo G., Manfredi G. Nonlinear Mechanical Model of Seismic Behaviour of Beam-Column Pin Connections. 15th World Conference on Earthquake Engineering, Lisbon: 2012.
[9] Rodrigues H., Sousa R., Batalha N., Vitorino H., Varum H., Fernandes P. Typical properties of the Portuguese precast industrial buildings. Advances in Civil Engineering 2020.
[10] Bellotti D., Casotto C., Crowley H., Deyanova M.G., Germagnoli F., Lucarelli E., et al. Capannoni monopiano prefabbricati: distribuzione proba- bilistica dei sistemi e sottosistemi strutturali dagli anni sessanta ad oggi Single-storey precast buildings: probabilistic distribution of structural systems and subsystems from the sixties 2014;5. https://doi.org/10.7414/PS.5.3.41–70.
[11] Senel S.M., Kayhan A.H. Fragility based damage assesment in existing precast industrial buildings: A case study for Turkey 2010;34:39–60.
[12] Sousa R, Batalha N, Silva V, Rodrigues H. Seismic fragility functions for Portuguese RC precast buildings. Bull Earthq Eng 2020;2020:1–18. https://doi.org/10.1007/S10518-020-01007-7.
[13] Behavior of Dowels Under Cyclic Deformations. ACI Struct J 1987;84. https://doi.org/10.14359/2749.
[14] Cimmino M, Magliulo G, Manfredi G. Seismic collapse assessment of new European single-story RC precast buildings with weak connections. Bull Earthq Eng 2020;18:6661–86. https://doi.org/10.1007/s10518-020-00952-7.
[15] Bosio M, Di Salvatore C, Bellotti D, Capacci L, Belleri A, Piccolo V, et al. Modelling and seismic response analysis of non-residential single-storey existing precast buildings in Italy. J Earthq Eng 2023;27:1047–68. https://doi.org/10.1080/13632469.2022.2033364.

[16] Batalha N, Rodrigues H, Arêde A, Furtado A, Sousa R, Varum H. Cyclic behaviour of precast beam-to-column connections with low seismic detailing. Earthq Eng Struct Dyn 2022:1–19. https://doi.org/10.1002/eqe.3606.
[17] Belleri A, Marini A, Riva P, Nascimbene R. Dissipating and re-centring devices for portal-frame precast structures. Eng Struct 2017;150:736–45. https://doi.org/10.1016/j.engstruct.2017.07.072.
[18] Morgen B.G., Kurama Y.C., Ph D. A Friction Damper for Post-Tensioned Precast Concrete n.d.
[19] Yildirim S., Kalyoncuoglu A., Erkus B., Tonguc Y. Seismic Retrofit of Industrial Precast Concrete Structures Using Friction Dampers: Case Study from Turkey. Second ATC & SEI Conference on Improving the Seismic Performance of Existing Buildings and Other Structures, San Francisco, California: 2015. https://doi.org/10.1061/9780784479728.057.
[20] Mohamed N, Shabir A, Jinkoo K. Self-centering steel slotted friction device for seismic retrofit of beam-column joints. Steel Compos Struct 2021;41:13–30. https://doi.org/10.12989/SCS.2021.41.1.013.
[21] Pollini AV, Buratti N, Mazzotti C. Experimental and numerical behaviour of dissipative devices based on carbon-wrapped steel tubes for the retrofitting of existing precast <scp>RC</scp> structures. Earthq Eng Struct Dyn 2018;47:1270–90. https://doi.org/10.1002/eqe.3017.
[22] Soydan C., Gullu A., Hepbostancı O.E., Yuksel E., Irtem E. Design of a Special Lead Extrusion Damper. 15th World Conference on Earthquake Engineering, Lisbon: 2012.
[23] Magliulo G, Cimmino M, Ercolino M, Manfredi G. Cyclic shear tests on RC precast beam-to-column connections retrofitted with a three-hinged steel device. Bull Earthq Eng 2017;15:3797–817. https://doi.org/10.1007/s10518-017-0114-x.
[24] Di Salvatore C., Magliulo G., Castellano M.G., Caterino N. SEISMIC RETROFITTING OF SINGLE-STORY RC PRECAST BUILDINGS THROUGH A NOVEL METALLIC HYSTERETIC DEVICE, 2021, p. 4789–4799. https://doi.org/10.7712/120121.8826.19461.
[25] Bressanelli ME, Bosio M, Belleri A, Riva P, Biagiotti P. Crescent-moon beam-to-column connection for precast industrial buildings. Front Built Environ 2021;7. https://doi.org/10.3389/fbuil.2021.645497.
[26] Rodrigues H, Sousa R, Batalha N, Vitorino H, Varum H, Fernandes P. Typical properties of the Portuguese precast industrial buildings. Adv Civ Eng 2020.
[27] Bournas D.A., Negro P. Seismic Performance of Mechanical Connections in the SAFECAST Precast Building 2003;3.
[28] Psycharis IN, Mouzakis HP. Assessment of the seismic design of precast frames with pinned connections from shaking table tests. Bull Earthq Eng 2012;10:1795–817. https://doi.org/10.1007/s10518-012-9372-9.